

Selective Imidazolidine Ring Opening during Complex Formation of Iron(III), Copper(II), and Zinc(II) with a Multidentate Ligand Obtained from 2-Pyridinecarboxaldehyde *N*-Oxide and Triethylenetetramine

M. Boča,^{*,†} P. Baran,[†] R. Boča,[†] H. Fuess,[‡] G. Kickelbick,[§] W. Linert,[§] F. Renz,^{||} and I. Svoboda[‡]

Department of Inorganic Chemistry, Slovak Technical University, SK-812 37 Bratislava, Slovakia, Institute of Materials Science, Darmstadt University of Technology, D-64289 Darmstadt, Germany, Institute of Inorganic Chemistry, Vienna University of Technology, A-1060 Vienna, Austria, and Institute of Inorganic and Analytical Chemistry, Johannes Gutenberg University, D-55099 Mainz, Germany

Received December 7, 1999

The condensation of 2-pyridinecarboxaldehyde *N*-oxide and triethylenetetramine yields a product with two imidazolidine rings, as proven by a solid-state X-ray structure analysis as well as by NMR solution spectra. This ligand, L¹, undergoes a ring-opening reaction on complex formation with Cu(II), yielding [CuL²]²⁺ where L² functions as a pentadentate ligand, containing only one imidazolidine ring. On complexation with Zn(II) and Fe(III), both rings are opened and the complexes [ZnL³]²⁺ and [FeL³]³⁺ with a hexadentate L³ ligand are formed. The recrystallization of [ZnL³]²⁺ from DMSO solution results in the complex [ZnL¹(DMSO)₂]²⁺ in which L¹ behaves as a tetradentate ligand. Thus L¹, L², and L³ are structural isomers with two, one, or no imidazolidine rings, as confirmed by X-ray structure analyses. The intramolecular ring formation is the result of the nucleophilic addition of the N(amino) group to the electrophilic sp²-hybridized –HC^{δ+}=N site. Owing to the absence of the chelate effect on the sp³-hybridized carbon atom belonging to the imidazolidine ring, the ring opening is facilitated and readily observed upon complex formation with Cu(II), Zn(II), and Fe(III).

Introduction

Condensation reactions of aromatic aldehydes with α,ω -polyamines may lead to various products, e.g., (i) if a polyamine with primary amino groups only is involved, a Schiff base arises by condensation,¹ (ii) condensation of the polyamines with secondary amino groups results in the imidazolidines,² and (iii) if the polyamine contains primary and secondary amino groups, the condensation products are Schiff bases, imidazolidines, or Schiff bases with additional imidazolidine rings.³ Cobalt(II), nickel(II), and barium(II) complexes are examples of such

products.⁴ An important feature of such isomerization reactions is the contraction/expansion of the metal ion containing inner ring.⁵

Imidazolidine ring formation and its cleavage are important in various fields: (i) in organic synthesis imidazolidines can act as protective groups, since they are particularly easy to hydrolyze in acidic solutions and are stable in basic solutions, (ii) nitroalkanes can be acylated with imidazolidines, and (iii) imidazolidines can act as intermediates in the biosynthesis of nucleotides.⁶

Results and Discussion

The product of the 2-pyridinecarboxaldehyde *N*-oxide reaction with triethylenetetramine (2:1 molar ratio) is the species L¹ (**I**): 2,2'-[1,2-ethanediy]bis(1,3-diazolidine-2-yl)]bis(1-oxopyridine). The reaction likely proceeds in two steps (Figure 1):

* Author for correspondence.

[†] Slovak Technical University.

[‡] Darmstadt University of Technology.

[§] Vienna University of Technology.

^{||} Johannes Gutenberg University.

- (1) (a) Rodley, G. A.; Robinson, W. T. *Nature* **1972**, 235, 438. (b) Avdeef, A.; Schäfer, W. P. *J. Am. Chem. Soc.* **1976**, 98, 5153. (c) Gall, R. S.; Schäfer, W. P. *Inorg. Chem.* **1976**, 15, 2759. (d) Gall, R. S.; Rogers, J. F.; Schäfer, W. P.; Christoph, G. G. *J. Am. Chem. Soc.* **1976**, 98, 5135. (e) Schäfer, W. P.; Huie, B. T.; Kurilla, M. G.; Ealick, S. E. *Inorg. Chem.* **1980**, 19, 340. (f) Boča, R.; Elias, H.; Haase, W.; Hüber, M.; Klement, R.; Müller, L.; Paulus, H.; Svoboda, I.; Valko, M. *Inorg. Chim. Acta* **1998**, 278, 127.
- (2) (a) Coleman, W. M.; Taylor, L. T. *J. Inorg. Nucl. Chem.* **1980**, 42, 683. (b) Yamamoto, Y.; Tsukuda, S. *Bull. Chem. Soc. Jpn.* **1985**, 58, 1509. (c) Maeda, Y.; Oshio, H.; Tanigawa, Y.; Onoki, T.; Takashima, Y. *Bull. Chem. Soc. Jpn.* **1991**, 64, 1522. (d) Evans, D. F.; Jakubovic, D. A. *J. Chem. Soc., Dalton Trans.* **1988**, 2927.
- (3) (a) Sarma, B. D.; Bailar, J. C., Jr. *J. Am. Chem. Soc.* **1954**, 76, 4051. (b) Ferm, R. J.; Riebsomer, J. L. *Chem. Rev.* **1954**, 54, 593. (c) Moos, F. *Ber. Dtsch. Chem. Ges.* **1887**, 20, 732. (d) Sarma, B. D.; Bailar, J. C., Jr. *J. Am. Chem. Soc.* **1955**, 77, 5476. (e) Riebsomer, J. L. *J. Org. Chem.* **1950**, 15, 237. (f) Ferm, R. J.; Riebsomer, J. L.; Martin, E. L.; Daub, D. H. *J. Org. Chem.* **1952**, 17, 643.

- (4) (a) Nelson, S. M.; Knox, C. V.; McCann, M.; Drew, M. G. B. *J. Chem. Soc., Dalton Trans.* **1981**, 1669. (b) Drew, M. G. B.; Nelson, J.; Nelson, S. M. *J. Chem. Soc., Dalton Trans.* **1981**, 1678. (c) Drew, M. G. B.; Nelson, J.; Nelson, S. M. *J. Chem. Soc., Dalton Trans.* **1981**, 1685. (d) Drew, M. G. B.; Nelson, J.; Nelson, S. M. *J. Chem. Soc., Dalton Trans.* **1981**, 1691.
- (5) (a) Adams, H.; Bailey, N. A.; Fenton, D. E.; Good, J. J.; Moody, R.; Cecilia, O.; de Barbarin, R. *J. Chem. Soc., Dalton Trans.* **1988**, 207. (b) Adams, H.; Bailey, N. A.; Bertrand, P.; Collinson, S. R.; Fenton, D. E.; Kitchen, S. J. *J. Chem. Soc., Dalton Trans.* **1996**, 1181. (c) Menif, R.; Martell, A. E.; Squattrito, P. J.; Clearfield, A. *Inorg. Chem.* **1990**, 29, 4723.
- (6) (a) Greene, T. W.; Wuts, P. G. M. *Protective Groups in Organic Synthesis*, 2nd ed.; Wiley: New York, 1991. (b) Staab, H. A. *Angew. Chem.* **1962**, 74, 407. (c) Baker, D. C.; Putt, S. R. *Synthesis* **1978**, 478. (d) Stryer, L. *Biochemistry*, 3rd ed.; Freeman: New York, 1988; p 603.

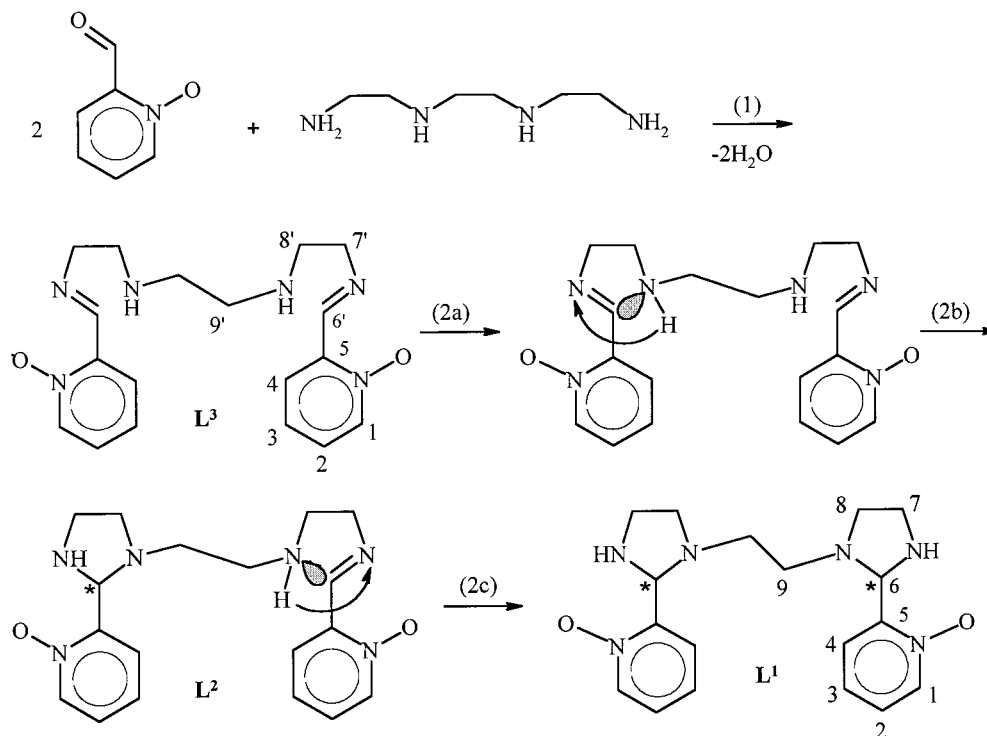


Figure 1. Synthetic route for the preparation of the isomers L^1 , L^2 , and L^3 (with labeling of the carbon atoms for analysis of the ^{13}C NMR spectra): (1) condensation; (2) nucleophilic addition preceded by hydrogen atom migration.

Table 1. Crystal Data and Structure Refinement Details for Compounds I–V

	I	II	III	IV	V
empirical formula	$\text{C}_{18}\text{H}_{24}\text{N}_6\text{O}_2$	$\text{C}_{18}\text{H}_{24}\text{Cl}_2\text{CuN}_6\text{O}_{10}$	$\text{C}_{18}\text{H}_{24}\text{Cl}_2\text{N}_6\text{O}_{10}\text{Zn}$	$\text{C}_{104}\text{H}_{144}\text{Cl}_8\text{N}_{24}\text{O}_{56}\text{S}_{16}\text{Zn}_4$	$\text{C}_{19}\text{H}_{24}\text{Cl}_3\text{FeN}_6\text{O}_{15}$
M	356.48	618.87	620.70	3684.74	738.69
color	colorless	violet	yellow	yellow	orange
cryst syst	triclinic	monoclinic	monoclinic	triclinic	orthorhombic
space group	$P1$	$P2_1/n$	$C2/c$	$P1$	$Pbcn$
$a/\text{\AA}$	5.229(1)	12.4955(1)	16.1788(2)	15.5916(1)	12.2942(2)
$b/\text{\AA}$	7.014(1)	13.0858(3)	11.7892(1)	15.8716(2)	16.5779(1)
$c/\text{\AA}$	12.473(2)	14.8529(3)	13.2215(2)	18.0336(1)	14.3698(3)
α/deg	87.68(2)	90	90	90.463(1)	90
β/deg	85.98(2)	98.580(2)	103.677(1)	110.229(1)	90
γ/deg	74.43(2)	90	90	93.632(1)	90
$V/\text{\AA}^3$	439.5(1)	2401.47(8)	2450.30(5)	4176.84(6)	2928.74(8)
T/K	304(2)	298(2)	293(2)	293(2)	293(2)
Z	1	4	4	1	4
$\lambda/\text{\AA}$	0.710 93	0.710 73	0.710 73	0.710 73	0.710 73
$\rho_{\text{calcd}}/(\text{Mg}/\text{m}^3)$	1.347	1.712	1.677	1.465	1.675
cryst size/mm	$0.40 \times 0.15 \times 0.05$	$0.35 \times 0.37 \times 0.40$	$0.42 \times 0.32 \times 0.30$	$0.35 \times 0.41 \times 0.37$	$0.24 \times 0.22 \times 0.14$
μ/mm^{-1}	0.054	1.199	1.286	0.980	0.869
hkl ranges	$-5, 2; -7, 7; -13, 13$	$-9, 17; -18, 18; -1, 21$	$-22, 23; -16, 16; -16, 18$	$-20, 22; -22, 21; -17, 25$	$-17, 13; -20, 23; -16, 20$
no. of data collected	1715	13 456	10 327	23 557	15 439
no. of indep reflns (R_{int})	817 (0.0564)	4238 (0.0550)	3731 (0.0210)	14 424 (0.0282)	2574 (0.0541)
$R(F)$ [$I > 2\sigma(I)$]/%	4.75	5.72	3.22	6.08	5.80
$R_w(F^2)$ (all data)/%	15.10	17.00	9.38	17.86	17.09
goodness of fit on F^2	1.032	1.030	1.039	1.091	1.079
largest peak and hole/ $e \text{\AA}^{-3}$	0.17, -0.20	0.86, -0.50	0.774, -0.407	0.722, -0.459	1.223, -1.079
no. of data, restraints, param	1221, 0, 167	4143, 0, 342	3728, 0, 169	13 641, 6, 1083	2505, 0, 249

the Schiff condensation, (1), and the nucleophilic addition of the nitrogen atom (secondary amine group) to the electrophilic $\text{C}^{\delta+}$ center, (2), accompanied by a hydrogen atom migration.

The structure of L^1 has been confirmed by a solid-state X-ray structure analysis (the crystal data for I are collected in Table 1, atomic coordinates and complete geometric parameters are contained in the Supporting Information, and selected bond lengths are listed in Table 2). The molecular structure of L^1 is presented in Figure 2. The critical bond length responsible for the imidazolidine ring formation/cleavage is $\text{C}(6)-\text{N}(3) = 1.474$

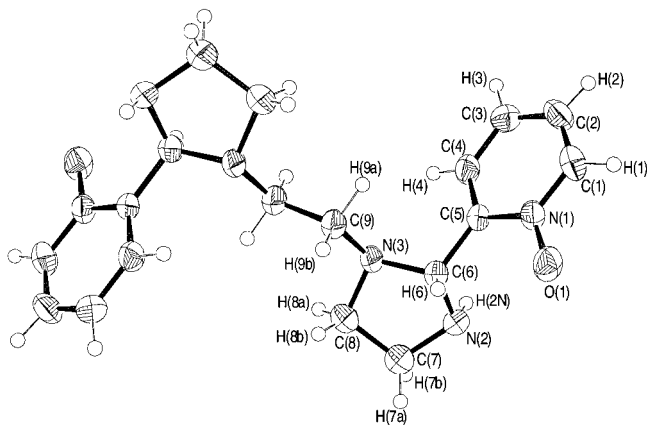
\AA . The pyridine rings in species L^1 are found to be nicely parallel.

Each molecule in I exhibits four intermolecular hydrogen bonds on the linkage, $\text{N}(2)-\text{H}(2\text{N})\cdots\text{O}(1)$ being nearly linear, with $\text{N}(2)-\text{H}(2\text{N}) = 0.929 \text{ \AA}$, $\text{N}(2)-\text{O}(1) = 2.982 \text{ \AA}$, and $\text{N}(2)-\text{H}(2\text{N})-\text{O}(1) = 172.8^\circ$. Just the hydrogen atom $\text{H}(2\text{N})$ migrates toward the $\text{N}(3)$ atom upon the imidazolidine ring cleavage.

Whether the form L^1 survives in solutions has been investigated by ^{13}C NMR spectroscopy (Table 3).⁷

Table 2. Selected Bond Lengths (Å) for Ligand **I** and Complexes **II–V**

	I		II		III		IVa		IVb		V	
C(1)–C(2)	1.3666(2)	Cu–O(20)	1.926(3)	Zn–O(10a)	2.108(1)	Zn(1)–O(1)	2.089(3)	Zn(2)–O(70)	2.079(3)	Fe–O(10)	1.868(3)	
C(1)–N(1)	1.3553(3)	Cu–N(14)	1.943(4)	Zn–O(10)	2.108(1)	Zn(1)–O(26)	2.102(3)	Zn(2)–O(65)	2.111(3)	Fe–O(10a)	1.868(3)	
C(2)–C(3)	1.3800(3)	Cu–N(13)	1.981(4)	Zn–N(20)	2.146(1)	Zn(1)–O(31)	2.104(3)	Zn(2)–O(66)	2.114(3)	Fe–N(18)	1.920(4)	
C(3)–C(4)	1.3651(3)	Cu–N(12)	2.034(4)	Zn–N(20a)	2.146(1)	Zn(1)–O(27)	2.128(3)	Zn(2)–O(40)	2.121(3)	Fe–N(18a)	1.920(4)	
C(4)–C(5)	1.3730(2)	Cu–O(10)	2.335(3)	Zn–N(18)	2.162(1)	Zn(1)–N(12)	2.159(4)	Zn(2)–N(54)	2.167(4)	Fe–N(30)	1.990(4)	
C(5)–C(6)	1.4913(3)	Cu–O(100)	2.689(4)	Zn–N(18a)	2.162(1)	Zn(1)–N(15)	2.190(4)	Zn(2)–O(51)	2.182(4)	Fe–N(30a)	1.990(4)	
C(5)–N(1)	1.3663(3)	O(10)–N(10)	1.325(5)	O(10)–N(11)	1.319(2)	O(1)–N(2)	1.331(5)	O(40)–N(41)	1.342(5)	O(10)–N(11)	1.351(4)	
C(6)–N(2)	1.4575(4)	O(20)–N(20)	1.340(5)	O(10a)–N(11a)	1.319(2)	N(25)–O(26)	1.336(5)	O(65)–N(64)	1.333(5)	O(10a)–N(11a)	1.351(4)	
C(6)–N(3)	1.4745(3)	N(11)–H(11)	0.897(2)	C(17)–N(18)	1.268(2)	O(27)–S(28)	1.515(3)	O(66)–S(67)	1.524(4)	N(18)–C(17)	1.270(6)	
C(7)–C(8)	1.5236(3)	N(12)–C(105)	1.526(6)	C(17a)–N(18a)	1.268(2)	S(28)–C(30)	1.770(5)	S(67)–C(69)	1.771(7)	N(18a)–C(17a)	1.270(6)	
C(7)–N(2)	1.4718(4)	N(14)–C(112)	1.267(7)			S(28)–C(29)	1.772(6)	S(67)–C(68)	1.775(7)	H(30)–O(42)	1.269	
C(8)–N(3)	1.4610(4)	O(103)–H(13)	2.1950			O(31)–S(32)	1.508(3)	O(70)–S(71)	1.517(3)	H(30)–O(42a)	2.5786	
C(9)–N(3)	1.4523(4)	O(101)–H(11)	2.2529			S(32)–C(34)	1.770(7)	S(71)–C(73)	1.782(6)			
N(1)–O(1)	1.3140(2)					S(32)–C(33)	1.778(7)	S(71)–C(72)	1.784(7)			
N(2)–H(2N)	0.9290(2)					N(15)–C(19)	1.502(6)	N(54)–C(58)	1.509(6)			
O(1)–H(2N)	2.0576(2)					N(12)–C(8)	1.513(7)	N(51)–C(47)	1.503(6)			
						C(19)–N(18)	1.461(7)	C(58)–N(57)	1.449(8)			
						C(8)–N(9)	1.444(7)	C(47)–N(48)	1.465(7)			
						H(9)–O(601)	2.191	H(48)–O(303)	2.358			
						H(18)–O(404)	2.413	H(57)–O(701)	2.289			

**Figure 2.** ORTEP view of **I**.

The most pronounced difference in the NMR shifts of the imidazolidine and Schiff-base entities involves the carbon atoms C6 and C6' (for atom labeling, see Figure 1): $\delta(\text{C6, imidazolidine}) = 75$ ppm and $\delta(\text{C6', Schiff base}) = 158$ ppm. The experimental shifts clearly indicate the presence of imidazolidine carbon atoms C6 (and thus the form L^1) in solution: $\delta(\text{C6, imidazolidine}) = 76$ ppm. In contrast to the ^{13}C NMR spectra, the ^1H NMR spectra show two magnetically different pyridine *N*-oxide structures that may arise as a result of the coexistence of diastereomers and enantiomers and their conformers.

Crystal Structure of $[\text{CuL}^2(\text{ClO}_4)](\text{ClO}_4)$, **II.** The routes for the preparation of the complexes along with their numbering are shown in Scheme 1. Crystal data and selected bond lengths for **II** are presented in Tables 1 and 2. The structure of **II** consists of one $[\text{CuL}^2(\text{ClO}_4)]^+$ unit connected to one perchlorate counteranion (Figure 3).

During the complexation of L^1 to copper(II), a ring opening occurs and the pentadentate N_3O_2 -donor ligand L^2 is formed. The chromophore $\{\text{CuN}_3\text{O}_2\text{O}'\}$ adopts the geometry of a distorted octahedron: the coordination number is $4 + 1 + 1$. The second axial position is occupied by the oxygen atom from the perchlorate group at a $\text{Cu}–\text{O}$ distance of 2.689 Å. The $\text{N}–\text{O}$ bonds in the complex are longer by 0.011 and 0.026 Å than those in the free ligand L^1 . The critical bond length inside the imidazolidine ring is $\text{N}(12)–\text{C}(105) = 1.526$ Å, and it is the longest $\text{N}–\text{C}$ contact for the series of the complexes under study.

The coordinated perchlorate group forms two additional hydrogen bonds, but the uncoordinated perchlorate shows no hydrogen-bond network. The first intramolecular hydrogen bond is formed by an amine hydrogen atom with the distance $\text{O}(103)–\text{H}(13) = 2.185$ Å and the angle $\text{O}(103)–\text{H}(13)–\text{N}(13) = 159^\circ$. The second hydrogen bond is formed via intermolecular contact of the imidazolidine hydrogen atom with the distance $\text{O}(101)–\text{H}(11) = 2.253$ Å and the angle $\text{O}(101)–\text{H}(11)–\text{N}(11) = 165^\circ$.

Conductometric measurements (Table 3) revealed that complex **II** is a 1:1 electrolyte in nitromethane (a low donor number solvent), which matches the X-ray structure. However, it behaves as a 1:2 electrolyte in water, since the water molecule can readily replace the semicoordinated perchlorate group.

Crystal Structure of $[\text{ZnL}^3](\text{ClO}_4)_2$, **III.** Crystal data and selected bond lengths for **III** are presented in Tables 1 and 2. The structure of **III** consists of one $[\text{ZnL}^3]^{2+}$ unit and two perchlorate counteranions (Figure 4).

The $\{\text{ZnN}_4\text{O}_2\}$ chromophore involves the hexadentate L^3 ligand in a slightly distorted octahedron. The pyridine *N*-oxide groups lie in almost parallel planes. No hydrogen-bond network has been identified.

Crystal Structure of $[\text{ZnL}^1(\text{DMSO})_2](\text{ClO}_4)_2 \cdot 2\text{DMSO}$, **IV.** Crystal data and selected bond lengths for **IV** are presented in Tables 1 and 2. The formula unit reads $\{[\text{Zn}(1)\text{L}^1(\text{DMSO})_2]–[\text{Zn}(2)\text{L}^1(\text{DMSO})_2](\text{ClO}_4)_4(\text{DMSO})_4\}$. The $\{\text{ZnN}_2\text{O}_2\text{O}'_2\}$ chromophore of a slightly distorted octahedron involves the tetradentate N_2O_2 -donor ligand L^1 along with two cis-positioned DMSO ligands (Figure 5).

The critical bond lengths inside the imidazolidine rings ($\text{N}(12)–\text{C}(8) = 1.513$ Å, $\text{N}(15)–\text{C}(19) = 1.502$ Å, $\text{N}(51)–\text{C}(47) = 1.503$ Å, $\text{N}(54)–\text{C}(58) = 1.509$ Å) are shorter than the corresponding bond in the complex **II** ($\text{N}(12)–\text{C}(105)$), but they are still the longest $\text{N}–\text{C}$ contacts in complex **IV**.

A hydrogen-bond network has also been observed in analogy to complexes **II** and **V**. Each molecule of the ligand binds via its imidazolidine hydrogen atom to one perchlorate molecule and to one molecule of DMSO. The hydrogen bonds to DMSO are shorter ($\text{H}(9)–\text{O}(601) = 2.191$ Å, $\text{H}(57)–\text{O}(701) = 2.289$ Å) than the hydrogen bonds to the perchlorate groups ($\text{H}(18)–\text{O}(404) = 2.413$ Å, $\text{H}(48)–\text{O}(303) = 2.358$ Å).

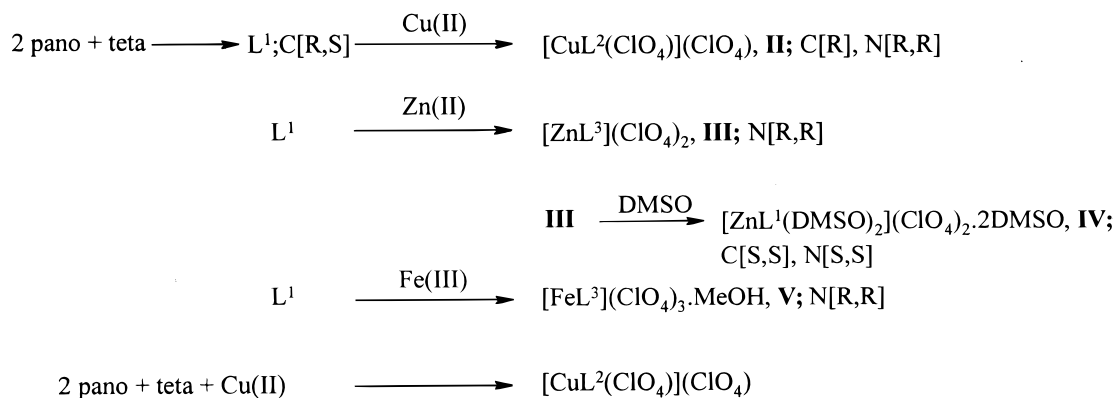
Upon dissolution of complex **III** in DMSO, complex **IV** is formed where ligand L^3 is altered to L^1 . In both cases and also

Table 3. Selected Experimental Data

system ^a	form	IR wavenumber/cm ⁻¹ ^b	¹³ C NMR shift δ /ppm (solvent) [predicted]	conductivity Λ /(Ω^{-1} mol ⁻¹ cm ²) (solvent), electrolyte	hardness η /eV; acceptor number A_N
I , L ¹	single crystal	$\nu(-C=N)$, missing $\nu(C-N_{py})$, 1609 w	C(6), 76.2, 75.9 (CDCl ₃) [C(6)H, 74.9 \pm 6.6] C(7), 44.4 (CDCl ₃) [C(7)H ₂ , 41.4 \pm 0.6]		
L ²	hypothetical		[C(6)H, 74.9 \pm 6.6] [C(7)H ₂ , 41.4 \pm 0.6] [-C(6')=, 158.5 \pm 3.6]		
L ³	hypothetical		[C(7')H ₂ , 58.4 \pm 5.1] [-C(6')=, 158.5 \pm 3.6] [C(7)H ₂ , 58.4 \pm 5.1]		
II , [CuL ² X]X	single crystal	$\nu(-C=N)$, 1638 m $\nu(C-N_{py})$, 1609 m		128 (CH ₃ NO ₂), 1:1 203 (H ₂ O), 1:2	Cu ²⁺ , 8.3; 61
III , [ZnL ³]X ₂	single crystal	$\nu(-C=N)$, 1655 s $\nu(C-N_{py})$, 1603 s		70 (DMSO), 1:2 318 (ACN), 1:2	Zn ²⁺ , 10.9; 70
IV , [ZnL ¹ (DMSO) ₂]X ₂	single crystal		C(6), 75.9 (DMSO) [C(6), 74.9 \pm 6.6] C(7), 43.1 (DMSO) [C(7)H ₂ , 41.4 \pm 0.6]		
V , [FeL ³]X ₃	single crystal	$\nu(-C=N)$, 1630 m $\nu(C-N_{py})$, 1611 s		381 (ACN), 1:3	Fe ³⁺ , 13.1; 69
VI , CoL ² X ₂	powder	$\nu(-C=N)$, 1625 m $\nu(C-N_{py})$, 1606 m			Co ²⁺ , 8.2; 57
VII , FeL ¹ X ₂	powder	$\nu(-C=N)$, missing $\nu(C-N)$, 1611 s			Fe ²⁺ , 7.3; 59

^a X⁻ = ClO₄⁻. ^b s = strong; m = medium; w = weak.

Scheme 1. Preparation of the Complexes Showing the Assignments of the *R*- and *S*-Configurations of the Chiral Centers



in an acetonitrile solution of **III**, the perchlorate groups do not coordinate and the conductivities for 1:2 electrolyte are observed.

Crystal Structure of [FeL³](ClO₄)₃·CH₃OH, V. Crystal data and selected bond lengths for **V** are presented in Tables 1 and 2. The structure of **V** consists of one [FeL³]³⁺ unit (analogous to **III**) and three perchlorate counteranions (Figure 6).

The {FeN₄O₂} chromophore involves the hexadentate L³ ligand in a slightly distorted octahedron. The N–O bonds in complex **V** are longer by 0.037 Å than those in L¹, and they are the longest N–O bonds of the studied complexes (this is a consequence of the higher positive charge on the Fe(III) center). In contrast to those of **III**, the pyridine *N*-oxide groups lie in perpendicular planes.

The ligand forms two hydrogen bonds via amino hydrogen atoms and oxygen atoms from distorted perchlorates with the distances H(30)–O(42) = 2.127 Å and H(30)–O(42a) = 2.579 Å, respectively, and angles H(30)–O(42)–N(30) = 178° and H(30)–O(42a)–N(30) = 170°.

Complex **V** behaves as a 1:3 electrolyte in acetonitrile, since the donor atoms of L³ occupy all six positions of the octahedron.

NMR Spectra of [ZnL³](ClO₄)₂, III. The ¹³C NMR spectra show (Table 3) that equivalent pyridine *N*-oxide moieties and equivalent imidazolidine rings exist in a solution of **III** in DMSO-*d*₆. Thus the L³ ligand present in the solid compound **III** undergoes a structural isomerization and the [ZnL¹]²⁺ complex exists in the DMSO solution, hereafter as **IIIb**, similar to the solid compound **IV**. These data show that the structural isomerization L¹(tetradentate) \rightleftharpoons L³(hexadentate) is facile.

The ¹H NMR spectra show some splitting: for example, the shift δ_H = 5.6 ppm appears as a 10 Hz doublet. The CH-COSY spectrum shows that δ_C = 76 ppm is correlated to δ_H = 5.6 ppm and thus the C*(6)–H(6) moiety is identified. The HH-COSY spectrum shows a correlation between $\delta_{H(C6)} = 5.6$ and $\delta_H = 4.1$ ppm. No correlation of a δ_C to $\delta_H = 4.1$ ppm was found in the CH-COSY spectrum, so that $\delta_{H(N)} = 4.1$ ppm should be assigned to the N–H moiety as shown in Figure 7.⁸ Then the doublet at $\delta_H = 5.6$ ppm, with the coupling constant

(8) Proton exchange in D₂O surprisingly exhibited no reduction of the N–H proton shift. Usually the acidic centers, such as N–H, exhibit a high exchange rate in protic solvents, such as DMSO + H₂O (minor). Their signal is averaged with the background and no resolution is obtained with multiscan FT-NMR spectroscopy.

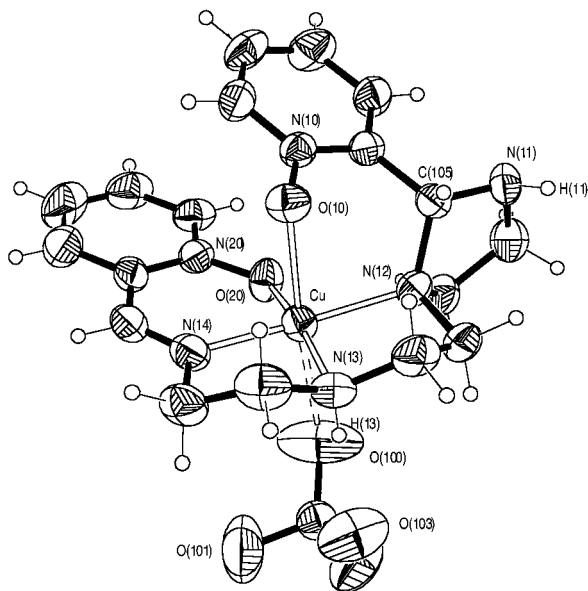


Figure 3. ORTEP view of **II**.

$J = 10$ Hz, arises from the vicinal protons $C^*(6)H-NH$. Such a coupling is unusual, since acidic centers exhibit a high exchange rate in protic solvents (which cannot be observed by the usual accumulation measurements, e.g., multiscan FT-NMR, because they constantly change their environment).

In terms of the Karplus equation, such a high value for the vicinal H–H coupling corresponds to a torsion angle of either 0 or 180°. A theoretical modeling shows that the equilibrium geometry of *rac*-[ZnL¹]²⁺ possesses torsion angles of 16° ([*R,R*] and/or [*S,S*] centers involved), whereas the corresponding values for the meso form [*R,S*] are 17° (*R* center) and 72° (*S* center).¹⁰ This supports the presence of only the *rac* form.

Chirality. Because all of our compounds crystallize in centrosymmetric space groups, they show no optical activity in the solid state despite the presence of the chiral centers. An overview of the chiral centers present in the single crystals is shown in Scheme 1.

Ligand **I** has two chiral carbon atoms: C(6) and C(6a). Inspection of the crystal structure shows that only the meso form [*R,S*] is present in the solid state. On complexation with Zn(II) and Fe(III), chirality of the carbon atoms of L³ in **III** and **V** is lost as a consequence of the ring opening and a reappearance of the Schiff base. The chirality of the amino nitrogen atoms was acquired by coordination to the central atom: complex **III** has two chiral centers, N(20)-[*R*] and N(20a)-[*R*]; in complex **V**, two chiral centers are present, N(30)-[*R*] and N(30a)-[*R*]. Recrystallization of **III** from DMSO yields **IV**, in which both zinc centers in the independent unit contain L¹ ligands with four chiral centers: C(8)-[*S*], C(19)-[*S*], N(12)-[*S*], N(15)-[*S*]; C(47)-[*S*], C(58)-[*S*], N(51)-[*S*], N(54)-[*S*]. Complex **II** contains three chiral centers: C(105)-[*R*], N(12)-[*R*], N(13)-[*R*].

IR Spectra. N–O stretching vibrations for **I** occur at 1234–1239 cm⁻¹ and are sensitive to coordination: for all complexes, these are shifted by ~30–40 cm⁻¹ to lower wavenumbers.⁷

A single N–H stretching vibration for **I** was observed at 3232 cm⁻¹, indicating that a symmetric L¹ molecule with imidazoli-

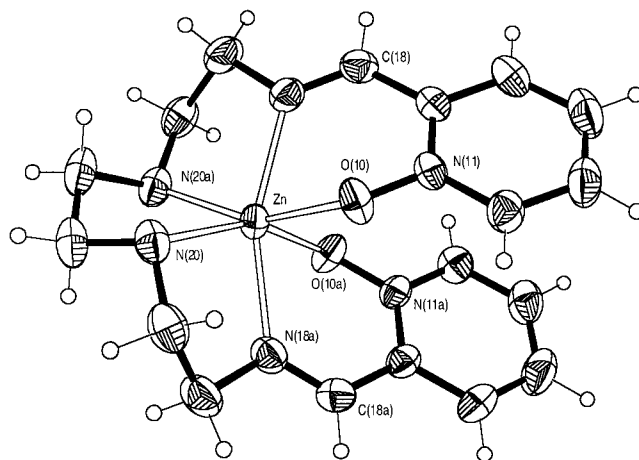


Figure 4. ORTEP view of **III**.

dine rings is formed; this is supported by the absence of the C=N vibration of a Schiff base (Table 3).

Two intense N–H stretching vibrations for **II** were observed. The first (at 3359 cm⁻¹) belongs to the aliphatic N–H secondary group and the second (at 3235 cm⁻¹) to the cyclic N–H secondary group. Analogously, two N–H stretching vibrations can be observed for the Co(II) complex **VI**,¹¹ suggesting the presence of ligand L². One N–H stretching vibration and one C=N vibration of a Schiff base were observed for Zn(II) complex **III** and Fe(III) complex **V**, corresponding to ligand L³. In the spectrum of the Fe(II) complex **VII**, one N–H and no Schiff base vibrations suggest the presence of L¹.

Imidazolidine Ring Closing/Cleavage. The formation of the imidazolidine ring occurs as a result of the nucleophilic addition of the amino N^{δ-} atom to the electrophilic C^{δ+} center of the Schiff base. Such a reaction is accompanied by hydrogen atom migration (Figure 1). This process exhibits some similarities to the nucleophilic additions observed in metal-assisted reactions of some pseudohalides of the nitrile class.^{12,13} Intramolecular nucleophilic addition associated with hydrogen atom migration has also been observed: cyanate reacts with dimethylpyrazole (dmpz) in the coordination sphere of Cu(II), and an extended Cu chelate is formed.¹⁴ In all these examples, the sp²-hybridized carbon β-site becomes an sp³-hybridized center and the gain in the conjugation energy stabilizes the chelate product. In our case, however, the sp²-hybridized Schiff-base carbon site becomes an sp³-hybridized imidazolidine center and no extra gain in the conjugation energy exists. Thus, the back transformation, or the equilibrium L¹(tetradentate) ⇌ L²(pentadentate) ⇌ L³(hexadentate), could be metal and solvent dependent. In fact, DMSO

(11) Also complexes of L² with Co(II) and L¹ with Fe(II) of the following compositions were prepared: CoL²(ClO₄)₂(H₂O), **VI** (brown), and FeL¹(ClO₄)₂(EtOH)_{0.5}(H₂O)_{0.5}, **VII** (green). Full characterization and other experiments will be published elsewhere.

(12) (a) Boča, R.; Hvastijová, M.; Koříšek, J.; Valko, M. *Inorg. Chem.* **1996**, *35*, 4794. (b) Hvastijová, M.; Koříšek, J.; Kohout, J.; Jäger, L. *J. Coord. Chem.* **1995**, *36*, 195. (c) Jamnický, M.; Segla, P.; Koman, M. *Polyhedron* **1995**, *14*, 1837. (d) Segla, P.; Jamnický, M.; Koman, M.; Glowiak, T. *Polyhedron* **1998**, *17*, 2765. (e) Dunaj-Jurčo, M.; Mikloš, D.; Potočník, I.; Jäger, L. *Acta Crystallogr.* **1996**, *C52*, 2409. (f) Boča, R.; Hvastijová, M.; Koříšek, J. *J. Chem. Soc., Dalton Trans.* **1995**, 1921. (g) Hvastijová, M.; Kohout, J.; Koříšek, J.; Boča, R.; Buchler, J.; Jäger, L. *Coord. Chem. Rev.* **1998**, *175*, 17.

(13) Cotton, F. A.; Daniels, L. M.; Haefner, S. C.; Kühn, F. E. *Inorg. Chim. Acta* **1999**, *287*, 159.

(14) (a) Kohout, J.; Valach, F.; Hvastijová, M.; Dunaj-Jurčo, M.; Gão, J. *J. Chem. Soc., Chem. Commun.* **1976**, 903. (b) Valach, F.; Kohout, J.; Dunaj-Jurčo, M.; Hvastijová, M.; Gão, J. *J. Chem. Soc., Dalton Trans.* **1979**, 1867. (c) Boča, R.; Hvastijová, M.; Kohout, J. *J. Coord. Chem.* **1994**, *33*, 137.

(9) (a) Karplus, M. *J. Chem. Phys.* **1959**, *30*, 11. (b) Karplus, M. *J. Am. Chem. Soc.* **1963**, *85*, 2870.

(10) A geometry optimization of the model complexes *rac*-[ZnL¹]²⁺ and *meso*-[ZnL¹]²⁺ has been performed using the density functional approach (B3LYP functional with lan12dz basis set) as implemented in the Gaussian-94 package. The *rac* form is found more stable by 0.0194 hartree.

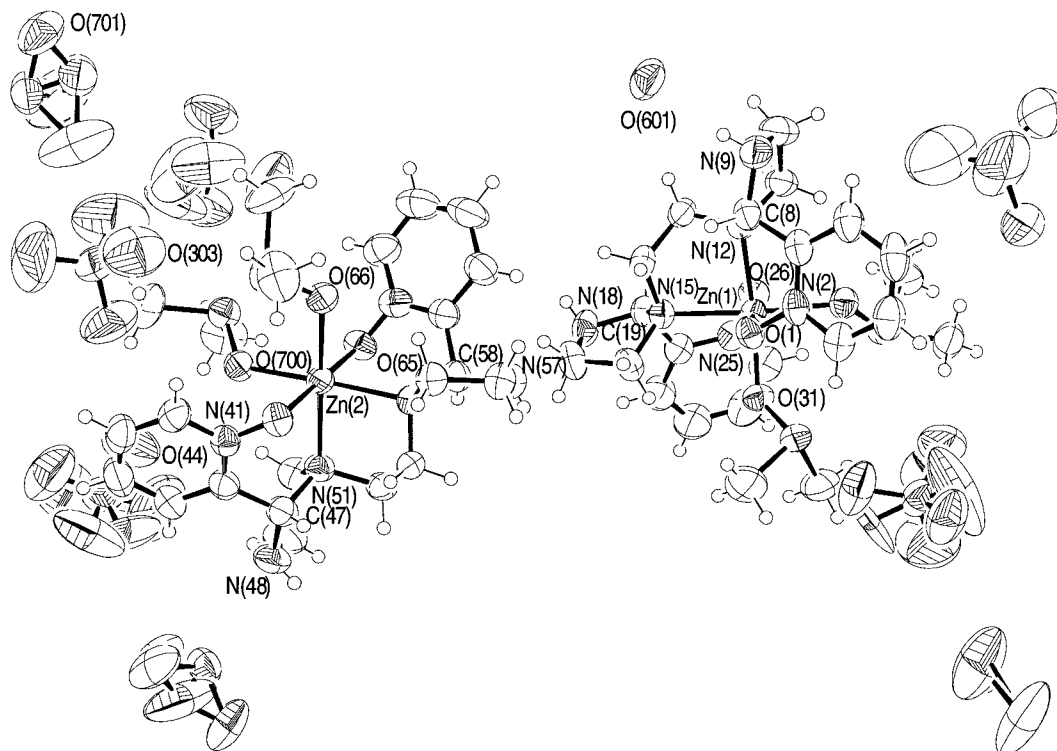


Figure 5. ORTEP view of the unit cell contents of IV.

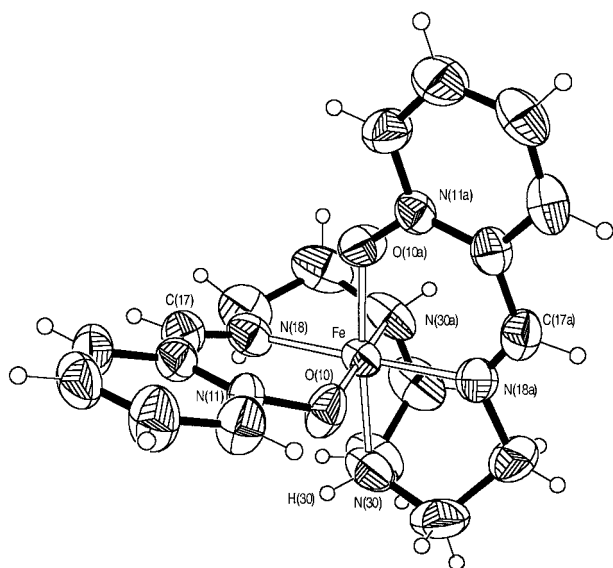


Figure 6. ORTEP view of V.

(a strongly coordinating agent, donor number $D_N = 29.8$) enters the coordination sphere of Zn(II) and prevents the presence of the L^3 (hexadentate) form, so that the ligand is back-transformed to its L^1 (tetradentate) isomer in IV.

Opening of the imidazolidine rings during complexation can be discussed in terms of the hardness (η ; Pearson)¹⁵ and eventually less common acceptor number (A_N ; Gutmann)¹⁶ of the central atom. The data in Table 3 show that a correlation exists between the Pearson hardness and the L^1 , L^2 , or L^3 isomer form: the greater the hardness of the central atom M (which serves as a measure of the Lewis acidity), the greater the preference to form an $[ML^3]$ complex with the hexadentate ligand L^3 . In terms of the HSAB (hard-soft acid-base) principle, the L^1 form would span a class of soft bases whereas L^3 would belong to a class of hard bases.¹⁵

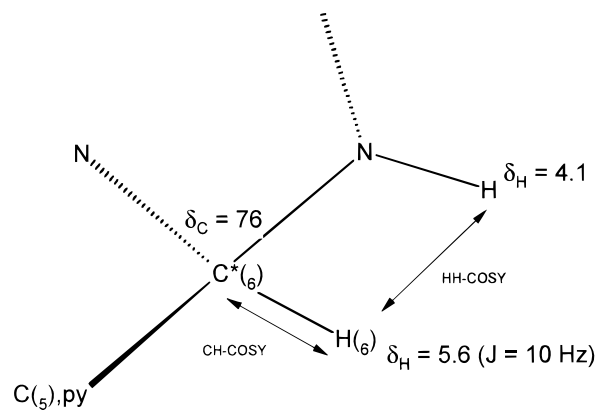


Figure 7. Atom labeling for a detailed analysis of the NMR data for IIIb.

Our proposition for the mechanism is as follows. After the condensation reaction, the Schiff base is ready for a nucleophilic attack via $-NH-$ units. In the absence of metal ions, the only

- (15) (a) Pearson, R. G. *J. Am. Chem. Soc.* **1963**, *85*, 3533. (b) Parr, R. G.; Pearson, R. G. *J. Am. Chem. Soc.* **1983**, *105*, 7512. (c) Komorowski, L. *Chem. Phys. Lett.* **1987**, *134*, 536. (d) Sen, K. D., Ed. *Structure Bonding*; Springer: Berlin, 1993; Vol. 80. The Pearson absolute hardness was identified by the HOMO-LUMO gap. A molecular modeling has been done using the parametrized AM/1 variant of MO calculations (starting set of atomic coordinates for L^1 and L^3 was retrieved from the X-ray data for I, III, and V). The total molecular energy in the optimum geometry of L^1 has been found only a bit lower than that of the L^3 form; the L^1 form is further stabilized via the hydrogen bonds in the solid state whereas L^3 is stabilized by the coordination to strong Lewis acids such as Fe^{3+} and Zn^{2+} . The closed form L^1 and the open form L^3 have comparable HOMO-LUMO gaps: between 8.2 and 8.6 eV, spanning the interval of intermediate hardness.
- (16) (a) Gutmann, V. *The Donor-Acceptor Approach to Molecular Interactions*; Plenum Press: New York, 1978. (b) Gutmann, V.; Henne, E. *Anorganische Chemie*, 5th ed.; VCH: Weinheim, Germany, 1990; p 203. (c) Linert, W.; Jameson, R. F.; Bauer, G.; Taha, A. *J. Coord. Chem.* **1997**, *42*, 211.

electrophilic center is the $-C=N-$ site of the Schiff base itself and thus the formation of L^1 is facile. In the presence of metal ions, the acidity of the $-C=N-$ site competes with the acidity of the attacking central atom. Weak Lewis acids (such as Fe^{2+} , Co^{2+} , and Cu^{2+}) are incapable (or only partly capable) of splitting the imidazolidine ring whereas strong Lewis acids (e.g., Fe^{3+} and Zn^{2+}) can readily do so with the gain of the hexadenticity of L^3 .

Experimental Section

Equipment. Room-temperature conductivity measurements were performed using a B642 autobalance universal bridge (Wayne Kerr); corrections to the conductivity of pure solvents were applied.

IR spectra were measured in the 200–4000 cm^{-1} range on a PU 9800 FTIR spectrometer (Perkin-Elmer) for Nujol suspensions at room temperature.

1H and ^{13}C NMR spectra were recorded on an AC 250 FT spectrometer (Bruker) with a working frequency of 250 MHz using 1% TMS as an internal standard. Two-dimensional spectra were scanned for the zinc(II) complex by use of homonuclear-correlated spectroscopy (HH-COSY) and heteronuclear-correlated spectroscopy (CH-COSY). For NMR spectral studies, HPLC grade and deuterated NMR solvents were used as received.

Syntheses. All starting compounds and solvents were used as commercial products of analytical grade without any purification. 2-Pyridinecarboxaldehyde *N*-oxide was prepared according to the literature procedure.¹⁷

Preparation of Ligand L^1 (I). A solution of 5.99 cm^3 (40 mmol) of triethylenetetramine in methanol (10 cm^3) was added to a hot filtered solution of 10.08 g (80 mmol) of 2-pyridinecarboxaldehyde *N*-oxide in methanol (75 cm^3) under stirring. The mixture was stirred and heated on a water bath for 15 min. It was then cooled to room temperature and left to evaporate spontaneously to a volume of 35 cm^3 . Diethyl ether (150 cm^3) was added dropwise to the reaction mixture until a white solid began to precipitate. Then additional diethyl ether (400 cm^3) was added under stirring. After 20 min, the white product was filtered off, washed with diethyl ether, and air-dried. Yield: 7.8 g (53%). Mp: 166–167 °C. Anal. Calcd for $C_{18}H_{24}N_6O_2 \cdot 0.5H_2O$: C, 59.2; H, 6.89; N, 23.0. Found: C, 58.7; H, 6.62; N, 22.9. $\delta(HOH) = 1655\text{ cm}^{-1}$. The product was soluble in $CHCl_3$, alcohols, acetonitrile, pyridine, and DMSO and insoluble in diethyl ether. After dissolution in nitromethane, acetone, and water, marked color changes of the solutions were observed, resulting from reactions of the ligand with the solvents. After complexation, no visible color changes were observed during dissolution of the complexes in these three solvents. Single crystals of **I** suitable for X-ray determination were obtained by recrystallization of a powder sample from a 1:5 mixture of DMSO/MeOH.

Preparation of $[CuL^2(ClO_4)](ClO_4)$, Complex II. A solution of 0.3706 g (1 mmol) of $Cu(ClO_4)_2 \cdot 6H_2O$ in methanol (15 cm^3) was slowly added to a solution of 0.3564 g (1 mmol) of ligand in methanol (15 cm^3) under stirring at room temperature. A solid immediately precipitated. After 10 min of stirring, the dark violet product was filtered off, washed with methanol, and air-dried. Yield: 0.56 g (85%). Mp: 225–228 °C. Anal. Calcd for $C_{18}H_{24}N_6Cl_2CuO_{10} \cdot H_2O$: C, 34.0; H, 4.11; N, 13.2; Cu, 9.98; Cl, 11.1. Found: C, 34.3; H, 3.74; N, 13.0; Cu, 10.1; Cl, 12.2. $\delta(HOH) = 1672\text{ cm}^{-1}$.

The second method was a template reaction: A solution of 0.075 cm^3 (0.5 mmol) of triethylenetetramine in methanol (2 cm^3) and a solution of 0.185 g (0.5 mmol) of $Cu(ClO_4)_2 \cdot 6H_2O$ in methanol (2 cm^3) were added to a solution of 0.124 g (1 mmol) of 2-pyridinecarboxaldehyde *N*-oxide in methanol (8 cm^3) under stirring. After 3 h, the product of the same violet color was filtered off, washed with methanol, and air-dried. The compound was soluble in water, DMSO, acetonitrile, and methanol and insoluble in chloroform and diethyl ether. Single crystals of **II** suitable for X-ray analysis were obtained by recrystallization of a powder sample from acetonitrile.

Preparation of $[ZnL^3](ClO_4)_2$, Complex III. The cream-yellow zinc complex was prepared by the same method as used for the first preparation of the copper analogue (reaction time 5 h). Yield 0.42 g (62%). Mp: 237–239 °C. Anal. Calcd for $C_{18}H_{24}N_6Cl_2ZnO_{10}$: C, 34.7; H, 4.02; N, 13.5; Cl, 11.4; Zn, 11.5. Found: C, 35.2; H, 4.14; N, 13.4; Cl, 12.0; Zn, 11.7. $\delta(HOH)$: missing. The compound was soluble in water, DMSO, acetonitrile, and methanol and insoluble in chloroform and diethyl ether. Single crystals of **III** suitable for X-ray analysis were obtained by recrystallization of a powder sample from acetonitrile.

Preparation of $[ZnL^1(DMSO)_2](ClO_4)_2 \cdot 2DMSO$, Complex IV. This compound was prepared by recrystallization of **III** from DMSO.

Preparation of $[FeL^3](ClO_4)_3 \cdot CH_3OH$, Complex V. A solution of 0.5344 g (1 mmol) of $Fe(ClO_4)_3 \cdot 10H_2O$ in ethanol (15 cm^3) was slowly added to a solution of 0.3564 g (1 mmol) of ligand in ethanol (5 cm^3) under stirring at room temperature. The brown solid that appeared became orange within 100 min under stirring. The mixture was filtered, and the filtrate was washed with ethanol and air-dried. Yield 0.45 g (51%). Dec pt: >260 °C. Single crystals of **V** suitable for X-ray analysis were obtained by recrystallization of a powder sample accomplished by ether diffusion to through a methanol/acetonitrile (2:1) solution. Some of the single crystals, which were obtained in good yield, were powdered and subjected to elemental analysis. Anal. Calcd for $C_{18}H_{24}N_6Cl_3FeO_{14} \cdot CH_3OH$: C, 30.7; H, 3.80; N, 11.3; Cl, 14.3. Found: C, 30.7; H, 3.37; N, 11.4; Cl, 13.9. $\delta(COH) = 1656\text{ cm}^{-1}$. The compound was soluble in water, DMSO, acetonitrile, and methanol and insoluble in chloroform and diethyl ether.

Crystal Data Collection for Ligand L^1 (I). A single crystal was mounted on a CAD4 diffractometer (Enraf Nonius) using graphite-monochromated Mo $K\alpha$ radiation. Intensities were recorded with an $\omega-2\theta$ scan technique. Corrections for Lorentz, polarization, and absorption effects (empirical, ψ scan) were applied. The unit cell was determined by least-squares refinement with 25 accurately measured reflections.

Crystal Data Collections for Complexes II–V. Single crystals were mounted on a SMART diffractometer (Siemens) with a CCD area detector. Graphite-monochromated Mo $K\alpha$ radiation was used for all measurements. The crystal-to-detector distance was 4.40 cm. In each case, a hemisphere of data was collected by a combination of three sets of exposures at 293 K. Each set had a different ϕ angle for the crystal, and each exposure required 20 s and covered 0.3° in ω . The data were corrected for polarization and Lorentz effects, and an empirical absorption correction (SADABS) was applied.^{18a} Cell dimensions were refined using all unique reflections.

Structure Determinations. The structures were solved by direct methods (SHELXS-86).^{18b} Refinement was carried out with a full-matrix least-squares method based on F^2 (SHELXL-93)^{18c} using anisotropic thermal parameters for all non-hydrogen atoms. Hydrogen atoms were inserted in calculated positions and refined as riding on the atoms to which they were attached.

Conclusions

The condensation reaction of 2-pyridinecarboxaldehyde *N*-oxide and triethylenetetramine does not result in the usual Schiff-base product; instead, the ligand L^1 , having two external imidazolidine rings, is formed in the solid state, as proven by an X-ray structure analysis. This form survives in solutions, as evidenced by its NMR spectra.

The ligand L^1 undergoes one ring opening upon complex formation with Cu(II), yielding a $[CuL^2]^{2+}$ type complex where L^2 functions as a pentadentate ligand. On complexation with Zn(II) and Fe(III), both rings are opened and the complexes $[ZnL^3]^{2+}$ and $[FeL^3]^{3+}$ are formed with a hexadentate L^3 ligand. Recrystallization of $[ZnL^3]^{2+}$ from a DMSO solution results in

(17) Jerchel, D.; Heider, J.; Wagner, H. *Justus Liebig's Ann. Chem.* **1958**, 613, 153.

(18) (a) Sheldrick, G. M. *SADABS: Empirical Absorption Corrections Program*; University of Göttingen: Göttingen, Germany, 1997. (b) Sheldrick, G. M. *SHELXS-86: Program for the Solution of Crystal Structures*; University of Göttingen: Göttingen, Germany, 1986. (c) Sheldrick, G. M. *SHELXL-93: Program for Crystal Structure Determination*; University of Göttingen: Göttingen, Germany, 1986.

the $[\text{ZnL}^1(\text{DMSO})_2]^{2+}$ complex in which L^1 behaves as a tetradentate ligand.

The forms L^1 , L^2 , and L^3 are structural isomers with two, one, or no external imidazolidine rings as proven by X-ray structure analysis. The intramolecular ring formation occurs as a result of nucleophilic addition of the N(amino) group to the electrophilic sp^2 -hybridized $-\text{HC}^{\delta+}=\text{N}$ site. Owing to the absence of a chelate effect on the sp^3 -hybridized carbon atom belonging to the imidazolidine ring, the ring opening is facilitated and readily observed upon complex formation with Cu(II), Zn(II), and Fe(III).

Acknowledgment. We are pleased to acknowledge the support of the Bilateral Slovak-German Program (Project SLA-

005-97) and the Slovak Grant Agency (Project 1/6083/99). Thanks are also expressed for support from the European Community (Project ERB-FMRX-CT98-0199) and from the Fonds der Chemischen Industrie and the Austrian Federal Ministry of Science and Transport (Project GZ 70.023/2-Pr/4/97).

Supporting Information Available: Listings of IR and NMR data, bond distances and angles, atomic coordinates, and equivalent isotropic displacement parameters. This material is available free of charge via the Internet at <http://pubs.acs.org>. X-ray crystallographic files, in CIF format, are available from the Cambridge Crystallographic Database.

IC9914037